

Role of Architecture on the Conformation, Rheology, and Orientation Behavior of Linear, Star, and Hyperbranched Polymer Melts.

1. Synthesis and Molecular Characterization

Semen B. Kharchenko[†] and Rangaramanujam M. Kannan*

Department of Chemical Engineering and Materials Science, Wayne State University, Detroit, Michigan 48202

Jeff J. Cernohous and Shivshankar Venkataramani

3M Corporate Research Laboratories, 3M Center, St. Paul, Minnesota 55144

Received September 6, 2002; Revised Manuscript Received November 13, 2002

ABSTRACT: Polymer architecture plays an important role in the solution, rheological, mechanical and processing behavior. In this series of two papers, we explore the role of branching, especially branch density, on the conformation and rheology of homopolymers. A series of model star-core hyperbranched polystyrenes (HBPS) with branch functionality, f , ranging from approximately 15 to 55, and branch molecular weight M_{br} of 5, 10, 20, and 50 kg/mol are synthesized and characterized via triple detection SEC³ for the molecular weight, polydispersity, intrinsic viscosity, and radius of gyration. Compared to linear polymers and symmetric stars with three and eight arms of the same total molecular weight, these polymers exhibit considerably lower radius of gyration, Mark–Houwink exponent, and intrinsic viscosity. The hydrodynamic radii of HBPS with the highest branch density ($f \approx 50$) are only about half the corresponding values of linear polymers of the same molecular weight, whereas this ratio is equal to 0.8 for symmetric stars. Our measurements suggest that HBPS have a very compact shape, high segmental density, and a starlike architecture. HBPS with branches shorter than the characteristic critical molecular weight exhibit a linear dependence of zero-shear viscosity on molecular weight, suggesting a lack of entanglements, and further indicating the starlike nature of the HBPS. Study of the rheology and flow birefringence of model polystyrenes will be presented in the following publication in this journal (*Macromolecules* 2003, 36, 407).

Introduction

Synthesis of polymers with branched architectures and the study of the effect of architecture on the flow behavior has been the subject of keen interest over the past few decades. Recent developments in synthesis, characterization, and applications have generated renewed interest in understanding the relationship between molecular architecture and macroscopic orientation behavior. The branching topology may vary from the relatively simple cases of comblike, starlike, and H-like polymers, to the more complex cases of hyperbranched polymers and dendrimers. Since the flow and the processing behavior are intimately affected by architecture, a systematic understanding of the role of architecture on the rheological and orientation behavior is vital.¹

Rheology of linear and symmetric star polymers has been well characterized,^{2–4} whereas dendrimers and hyperbranched polymers (HBP) are relatively new classes of polymers, which are still being explored.^{5–18} Hyperbranched polymers have generated renewed interest not only in polymer chemistry, but also in medicine, space, automotive, and electronics industries. Even though dendrimers are monodisperse materials with highly controlled molecular architecture and surface group chemistry, their synthesis is a relatively tedious and multistep process. In comparison, hyperbranched polymers are relatively inexpensive, but the branching architecture may not be as well-defined.

To understand the role of architecture, a systematic study investigating the behavior of new classes of materials such as dense multiarm symmetric stars and hyperbranched polymers in relation to the properties of simpler branching architectures is being undertaken. For example, the dynamics of *entangled* symmetric stars with relatively low branch density can be described using the length and the number of arms.^{2–4} On the other hand, dendrimers and some hyperbranched polymers appear to show distinctly different dynamics compared to symmetric stars and linear polymers.^{5–9} In a recent publication, we made an attempt to address the unique, quantitative stress-optic behavior of hyperbranched polystyrenes (HBPS).¹⁰ In this series of two papers, we investigate the role of architecture and branch density, on the solution properties, rheology, and flow birefringence of linear, symmetric star, and hyperbranched polymers. To correlate the properties of hyperbranched and linear polymers, we have custom-synthesized HBPS with controlled branch lengths. Symmetric stars of relatively low functionality are also characterized for comparison. Specifically, we characterize the size of molecules and their topology, using a combination of size-exclusion chromatography (SEC or GPC), viscometry (IV), and light scattering (LS). On the basis of polymer characterization, we suggest a model for the visualization of size and shape of the controlled branch length HBPS. A key aspect of this work is the use of HBPS, which are either unentangled or weakly entangled. This allows us to focus on the architecture related effects, as opposed to entanglement effects, which is the case in previous studies on symmetric stars.

* Corresponding author: E-mail: rkannan@che.eng.wayne.edu.

[†] Currently at Polymers Division, NIST, Gaithersburg, MD.

In the following paper, we describe how the architecture affects rheology and the orientation behavior of linear, symmetric star, and HBPS.¹⁰

Background

Synthesis. A breakthrough in the synthesis of materials with unique architecture and viscoelastic behavior occurred in 1978 when the first synthesis of a dendritic molecule was introduced by Vogtle.⁵ Subsequently, it was further developed by Tomalia,⁷ Frechet^{8,14} and others, who synthesized well-characterized model dendrimers of varying generations. Less well-controlled branched structures were first synthesized by Kim,⁶ who termed them “hyperbranched” polymer (HBP). These polymers could be synthesized in one step and possessed most of the characteristics of dendrimers.^{9,11–13} In early 1980s, Webster and co-workers¹⁵ developed group transfer polymerization process for synthesizing polymers with hyperbranched architecture. Conventional scheme for the synthesis of HBP is based on the polycondensation of AB_x-type of monomers, for all $x \geq 2$. However, such approach amounted to relatively random branching pattern and molecular weight distribution.¹⁶ To gain a better control of structural parameters of HBPS, such as branch length and the number of branches, polymerization of living chain reactions, proton-transfer and ring-opening multibranching polymerization, and other synthetic techniques are widely utilized.^{17,18} Among those, anionic synthesis is the most popular. The branch is initially grown by polymerization of monomers into the particular length with active ends. The “living” branch with active end is stable, as the rates for termination and chain transfer stages are generally very slow. Subsequent reactions with linking agents are a key factor in the synthesis of an actual model system with a desired molecular architecture.

Molecular Characterization. Since the earliest theoretical work done on the analysis of the conformation and topology of highly branched polymers,^{19,20} a challenging aspect in characterizing the HBP appears to be its molecular weight distribution, which is usually measured by SEC.^{21,22} The difficulty arises from the fact that the hydrodynamic volume of HBP is significantly lower than that of a linear polymer of the same total molecular weight, therefore making it unfeasible to implement the calibration curve obtained from the analysis of polymers with linear chains.^{23–26} To obtain information about the degree of branching, and to characterize the shape and size of HBP, IR and NMR spectroscopy, as well as small-angle X-ray (SAXS) and neutron scattering (SANS) techniques, have been used.^{27,28} Recently, the technique of triple-detection (or SEC³), involving simultaneous implementation of gel permeation chromatography (GPC), intrinsic viscosity (IV), and light scattering (LS), has offered a great opportunity for characterization of each fraction of a polymer to determine both its size and molecular weight independently.

The number of branches in symmetric stars, as well as their lengths, is found to profoundly affect their conformational and dynamic properties.^{29–31} In general, when the molecular conformation is relatively unperturbed Gaussian statistics could be applied.^{32,33} This is usually the case for long linear chains, since both chain ends are allowed to assume all possible configurations. However, when the allowable conformations of the chain

are restricted, the distribution is no longer Gaussian. In a star, dendrimer, or hyperbranched polymer, one of the chain ends is always fixed at a junction point. Therefore, the number of possible conformations of such a chain is limited. Moreover, the presence of other attached chains hinders the motion of the given chain even more. This effect is stronger near the center of a molecule and is weaker on its periphery. As a result, chain segments near the center of a branched molecule could be significantly overstretched, leading to unique conformational arrangements purely as a result of architecture.^{34–37} The lower segmental density of chains in the neighborhood of chain ends allows them to fluctuate relatively freely. The strength of the perturbation from the Gaussian conformation is, therefore, closely related to the number of branches and the branch length. Experiments and molecular simulations suggest that for a star polymer with as few as eight arms, the conditions of Gaussian statistics may not be met.^{38,39}

In this paper, we explore how the potential departure from Gaussian statistics could be reflected in the solution properties. Light scattering and intrinsic viscosity measurements have been widely used to measure radius of gyration ($\langle R_g^2 \rangle^{1/2}$), and viscometric radius (R_η) of polymers, respectively. The magnitude of the latter is found to be equal to the hydrodynamic radius (R_h), which is a measure of the translational diffusion coefficient (D_0) for highly branched polymers.⁴⁰ R_η relates to intrinsic viscosity $[\eta]$, and R_h to D_0 through Stokes–Einstein relations:⁴¹

$$R_\eta = (3[\eta]M)^{1/3}(10\pi N_A)^{-1/3} \quad (1)$$

$$R_h = kT(6\pi\eta_s D_0)^{-1} \quad (2)$$

where M is molecular weight, N_A is Avogadro's number, k is the Boltzmann constant, T is ambient temperature, and η_s is solvent viscosity.

To characterize the change in molecular dimensions in dilute solution, we evaluate the so-called “shrinking” factors, h and g :³¹

$$h = (R_\eta)_{Br}/(R_\eta)_L \quad (3)$$

$$g = (\langle R_g^2 \rangle)_{Br}/(\langle R_g^2 \rangle)_L \quad (4)$$

where the subscripts “Br” and “L” refer to the corresponding radii of branched and linear polymer of equal molecular weight, respectively. The h factor represents the difference in hydrodynamic size of branched polymer related to the hydrodynamic size of linear counterpart, whereas g -factor provides the information about the geometrical shrinkage/expansion of a molecule. In addition, another parameter (ρ) is used to characterize molecular compactness. It probes the difference between molecular geometry and its hydrodynamic dimensions due to the presence of numerous branches:

$$\rho = R_\eta/\langle R_g^2 \rangle^{1/2} \quad (5)$$

The Mark–Houwink coefficients can be deduced from simple fits of molecular weight dependence of intrinsic

viscosity, as shown previously in long-chain branched polyethylene⁴²

$$[\eta] = kM_w^a \quad (6)$$

where k and a are experimentally obtained Mark–Houwink coefficients.

A number of studies demonstrate that the molecular weight dependence of intrinsic viscosity of dendrimers reaches a maximum value and then starts decreasing with increasing generation number.^{9,14,25,26,37} The convex type of this dependence was explained through different rates of growth of molecular weight and hydrodynamic volume. Hyperbranched polymers, on the other hand, may not necessarily follow this trend, yet their intrinsic viscosity is found to be still significantly lower than the corresponding numbers for linear molecules. Mark–Houwink exponent of a HBP in a good solvent is smaller than 0.4, whereas for linear polymers, the exponent is always greater than 0.5.^{23,37}

The solution characterization is used not only as a tool to understand the role of architecture, but also as a way to evolve a model for the type of branched structure exhibited by the HBPS used in this study.

Materials and Methods

Synthesis of Model Polymer Systems. Linear Polymers. Nearly monodisperse linear polystyrenes standards of varying molecular weights (both above and below the entanglement molecular weight, $M_e = 18.1$ kg/mol⁴³) were purchased from Scientific Polymer Products, Inc. They were used as received.

Symmetric Stars. Low functionality symmetric stars ($f = 3$ and 8) with arm molecular length M_a comparable to that for the branches of HBPS were custom synthesized and purchased from Polymer Source, Inc. Arms of the stars were synthesized anionically using stoichiometric ratios of initiator (*sec*-BuLi) and styrene. Small amount of butadiene was added at the end of the reaction to “end cap” the resulting polystyrene. To induce the coupling of polymerized arms into the eight-arm star, synthesis of octafunctional linking agent was a necessary step in the polymerization. It was based on the catalytic reaction of tetravinylsilane and dichloromethylsilane. Termination of the reaction with the linking agent was achieved by adding methanol. Finally, the polymer star was precipitated into ethanol and dried under vacuum.

Star–Core Hyperbranched Polymers. Custom synthesis of controlled branch-length HBPS was based on styrene (99%), cyclohexane, and divinylbenzene (Aldrich Co.) and was performed in our laboratories. All monomers and solvents were purified by passage through a column of basic alumina (Brockmann I, Aldrich Chemical Co.), and subsequently purged with research grade argon (Oxygen Services Co.). These materials were then stored over basic alumina at -20 °C in an argon atmosphere for up to 1 week. *sec*-Butyllithium (1.3 M in cyclohexane, Acros) was used without purification and was stored at -20 °C.

Model hyperbranched polystyrenes having controlled-branch lengths were obtained using the following synthetic procedure. Styrene (50 mL, 0.44 mol) and cyclohexane (500 mL) were transferred via cannula into a 2 L two-necked round-bottomed flask fitted with a septum and magnetic stir bar. After that, the solution was purged with the dry argon for 10 min at room temperature. *sec*-BuLi was added dropwise (~ 0.05 mL) until a persistent orange-red tint, characteristic of polystyryllithium color, was witnessed. To control the branch length and branch number associated with the targeted randomly hyperbranched stars, the ratio of initiator/monomer/branching agent (divinylbenzene) was varied. For instance, to obtain 5K-HBPS, 7.0 mL (0.0091 mol) of the initiator had been introduced and stirred under argon for 2 h at room temperature until the orange-red colorization was developed. After *all* of the styrene

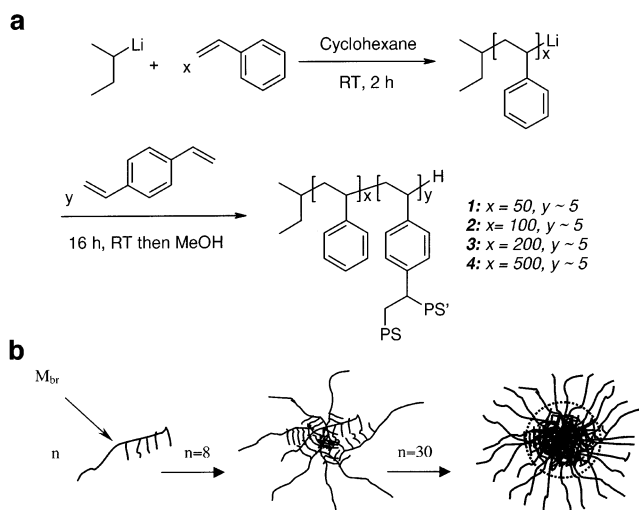


Figure 1. (A) Synthesis of model hyperbranched polystyrenes. (b) Schematic synthesis of HBPS.

monomer was consumed (as verified by the GPC analysis of an aliquot), divinylbenzene (5.0 mL, 0.042 mol) was charged into the flask. This approach of adding the branching agent *after* all the monomer had been consumed, was used to control the length of the branch. The homogeneous solution was then thoroughly mixed at room temperature for an additional 16 h to drive the coupling reaction until all available double bonds were consumed. Addition of degassed methanol (2 mL) to the flask quenched the polymerization. To precipitate the polymer, the solution was poured into excess 2-propanol (~ 2 L). The slurry was filtered and the polymer filtrate was purified by redissolution in THF (100 mL, Aldrich Co.), and reprecipitation in 2-propanol. The resulting material was collected via filtration and vacuum-dried at 60 °C for 3 h to yield 88% of white powder. Controlling the ratio of initiator to divinylbenzene, the rest of the hyperbranched polystyrenes were obtained (Figure 1a).

To get a better understanding of the architecture of HBPS, we offer a schematic representation (Figure 1b) of what architecture may emerge from the synthesis outlined above. Since the divinylbenzene is attached to only one end, the chains can come together only near the center (“divinylbenzene core”). This, coupled with the fact that the reaction was allowed to continue until all the double bonds were consumed, suggests that the procedure may result in a “starlike” polymer, with a relatively high functionality. In this schematic n is a desired number of branches of HBPS, and can vary from approximately 15 to 55. For clarity, a possible product of coupling first of eight and then of 26 such branches is shown. The mechanism of this reaction is likely to produce HBPS with numerous branches “sticking out” of what is considered to be a “core”. Table 1 lists important molecular characteristics of linear, symmetric star, and hyperbranched polymers obtained utilizing this synthetic procedure.

Molecular Characterization. To fully characterize the shape and size of a homopolymer, besides SEC, right-angle laser light scattering (RALLS) and intrinsic viscosity (IV) measurements are implemented. The technique of triple-detection involves simultaneous implementation of the three methods and allows for both the size and absolute molecular weight of each fraction to be determined. The RALLS detectors measure the intensity of light scattered from polymers in solution at different angles to independently determine the molecular weight, M_w , and viscometric radius, R_{η} . Additionally, molecular weight distributions and Mark–Houwink plots are obtained. A detailed experimental setup of the triple detection analysis is outlined below.

The SEC³ system consisted of a Waters Alliance 2690 HPLC system equipped with a precise solvent delivery system (pump), a degasser, and an auto-injector (Waters Corp.). The HPLC was operated at a flow rate of 1.0 mL/min, and the

Table 1. Molecular Characteristics of Model Polystyrenes

polymer architecture	M_w , g/mol	M_n , g/mol	PDI	est f	$[\eta]^*$, dL g ⁻¹	a (Mark–Houwink exponent)	$10^4\eta_0$, Pa s
Linear-PS							
5K-L-PS	5110	4800	1.07	2	0.049		0.008
13K-L-PS	13 100	12 200	1.07	2	0.096		0.077
19K-L-PS	19 000	17 800	1.07	2	0.126		0.17
61K-L-PS	61 800	58 300	1.06	2	0.298		6.18
171K-L-PS	171 000	164 400	1.04	2	0.626	0.73	106
393K-L-PS	393 400	339 100	1.16	2	1.148		851
1015K-L-PS	1 015 000	985 500	1.03	2	2.291		104 000
Symmetric Stars							
20K-3-arm	61 800	57 700	1.09	3			6.9
10K-8-arm	74 000	71 200	1.04	8	0.214		0.2
45K-8-arm	391 000	379 600	1.03	8	0.634	0.68	43.4
HBPS							
5K-HBPS	252 700	212 400	1.19	46–50	0.0915		3.0
10K-HBPS	575 600	456 800	1.26	45–57	0.127	0.39	6.7
20K-HBPS	960 700	313 000	3.07	15–50	0.336		13.4
50K-HBPS	1 264 000	730 700	1.73	15–25	0.462		37.8

^a Data for $[\eta]$ of L-PS are obtained from the power law $[\eta] = (9.6 \times 10^{-5})M_w^{-0.73}$ derived in our study.

injection volume for all samples was 0.1 mL. The columns used were 3×30 cm (7.5 mm diameter) each from a PLgel Mixed-B 10 μ m column set (Polymer Laboratories, Inc.). The triple detection system consists of a right-angle laser light-scattering system (RALLS) from Viscotek Corp. connected in series with a model 250 viscometer/refractive index detector also from Viscotek. Calibration of the light-scattering and refractive index detectors and the viscometer was performed with a narrow molecular weight distribution polystyrene standard purchased from American Polymer Standards with $M_w = 105\,200$ g/mol, $M_n = 99\,200$ g/mol, and an intrinsic viscosity of 0.465 dL/g in THF (Unstabilized, EM Science). The concentration of the samples was approximately 2.5 mg/mL. The mobile phase used was THF with a refractive index of 1.405. Given the high molecular weights of all of the model polymers (Table 1), the refractive index (RI) of these polymers would be expected to be practically molecular weight independent. The response of the RI detector is then a measure of the concentration of a solute in the effluent. The refractive index increment (dn/dc) could be dependent on molecular weight, and is expressed as: $dn/dc = a + b/M_n$, where a and b are constants and M_n is the number-average molecular weight. The larger the difference in RI between a solute and a solvent, the smaller the dependence of MW on dn/dc . Considering the relatively small RI difference between PS and THF, it may lead to a maximum of $\sim 5\%$ error in the light scattering molecular weights. The columns were maintained at 30 °C in an Eppendorf CH-60 column heater. All calculations were performed using the Viscotek TriSEC software (Version 3.00, Viscotek Corp.).

The radius of gyration, R_g of the HBPS was measured using a Wyatt DAWN EOS multiangle laser light scattering (MALLS) system. A polymer concentration of 1.0 mg/mL in mobile phase of toluene at a flow rate of 0.5 mL/min was used. The molecular weight distribution measured using the Wyatt system agreed reasonably well with the measurements using the SEC³ system. When comparisons of R_g and R_h of HBPS were made, the R_h measurements were also repeated in toluene (Table 2).

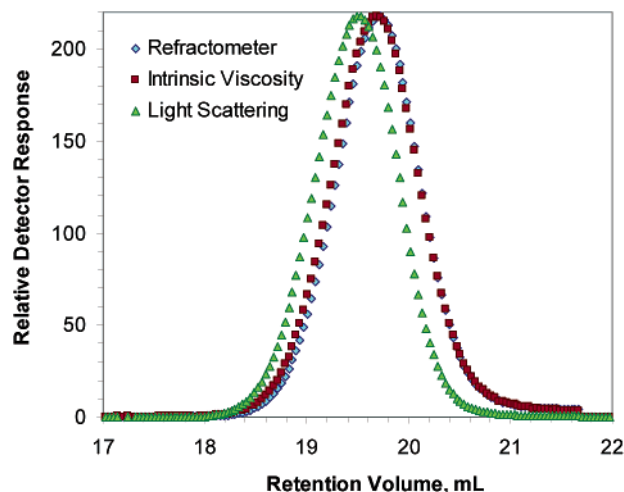
Results and Discussion

Molecular Weight Distribution. Using the SEC³ technique the molecular weight, molecular weight distribution, intrinsic viscosity ($[\eta]$), hydrodynamic radius (R_h), and the Mark–Houwink coefficients of the linear, star, and HBPS have been measured in a single set of experiments (Tables 1 and 2). The zero-shear viscosity based on melt rheology is also added in the last column of Table 1. To facilitate the analysis of the data, $[\eta]$ data for some of the linear polymers have been obtained from a power law fit using data from the measurements. The

Table 2. Evaluation of the “Shrinking” Factors g , h , and ρ for Model HBPS and Symmetric Stars^a

polymer	$\langle R_g^2 \rangle^{1/2}$, nm	R_h , nm	g	h	ρ
8.3K-L-PS	2.8	2.08	1	1	0.74
269.8K-L-PS	18.6	14.5	1	1	0.78
530.9K-L-PS	29.2	22.4	1	1	0.77
892.4K-L-PS	40.0	30.6	1	1	0.77
1206K-L-PS	50.4	36.7	1	1	0.73
5K-HBPS		7.1			0.48
10K-HBPS	10.0 ^b	10.5 (10.4 ^b)	0.104	0.44	1.043
20K-HBPS	16.0 ^b	17.2 (15.5 ^b)	0.148	0.53	0.971
50K-HBPS		20.9			0.56
8-arm-10K-star		6.0			0.81
8-arm-45K-star		14.5			0.75

^a To calculate g and h “shrinking” factors, data for R_h of L-PS of the same molecular weight as any of the branched polymer are extracted from eq 1, using intrinsic viscosity data of L-PS. Similarly, $\langle R_g^2 \rangle^{1/2}$ values for L-PS used for the comparison are obtained from the fit to the data in this table: $\langle R_g^2 \rangle^{1/2} = (1.48 \times 10^{-2})M_w^{0.58}$. ^b Measured in toluene.

**Figure 2.** Triple detection analysis of 10K-HBPS.

molecular weight data for the linear and symmetric stars are either measured or used as supplied by the manufacturer, which is indicated in the table. Triple detection chromatogram for one of the HBPS is shown in Figure 2, and the molecular weight distributions of all model HBPS are plotted in Figure 3. To compare the shapes of the molecular weight distribution, it is convenient to plot them against the reduced molecular

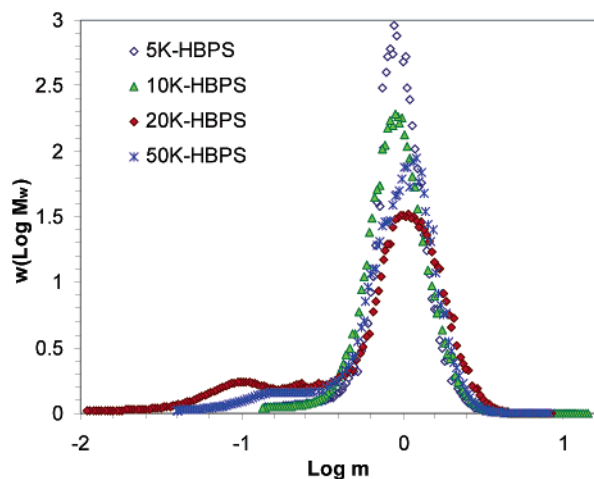


Figure 3. Comparison of the MWD for HBPS vs reduced molecular weight (m).

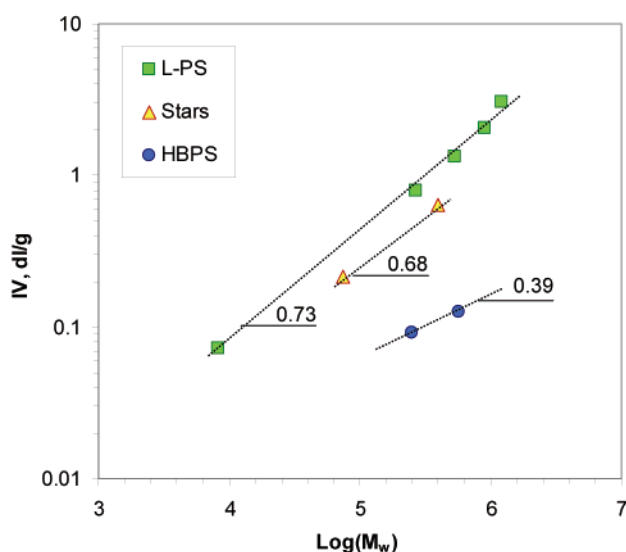


Figure 4. Effect of branching on the intrinsic viscosity (IV) in THF at $T = 30\text{ }^{\circ}\text{C}$. Symbols represent experimental data, and dashed lines represent linear fits.

weight m ($m = M/M_w$). Since the branches are first grown anionically and verified to be nearly monodisperse, the shapes of the curves would provide an idea of the extent of polydispersity in the number of arms in the HBPS. The molecular weight distributions for 5K-HBPS and 10K-HBPS are nearly monomodal with a PDI of 1.19 and 1.26, respectively (Table 1). The small polydispersity more likely represents the variation in the branch functionality (f). The distributions for the 20K-HBPS and 50K-HBPS are somewhat broader, which might correspond to a broader "branch polydispersity" in these polymers. The molecular weight distribution is used in conjunction with the intrinsic viscosity data to gain more insights into the branch functionality in these materials.

Intrinsic Viscosity. Signature plots of molecular weight dependence of intrinsic viscosities of linear, star, and hyperbranched polystyrene show the role of branch density on polymer hydrodynamic volume (Figure 4). We compare polymers of similar branching density; therefore, only two symmetric stars with $f = 8$ arms (10K-8-arm, 45K-8 arm) and two HBPS of the highest degree of branching ($f \approx 50$) (5K-HBPS and 10K-HBPS) are chosen. First, it is apparent that for the same total

molecular weight, $[\eta]$ decreases significantly for HBPS which have a high branch density. Dilute solutions of linear PS (THF, $T = 30\text{ }^{\circ}\text{C}$) show the following behavior:

$$[\eta]_L = (9.6 \times 10^{-5}) M_w^{0.73} \quad (7)$$

The Mark–Houwink exponent of 0.73 is consistent with previous results in good solvents.⁴⁴ On the other hand, symmetric PS stars (eight-arm) exhibit a somewhat lower value of $a = 0.68$ in the same solvent and at the same temperature. Even though only two HBPS with comparable, high branch density are fitted (5K- and 10K-HBPS), they show considerably lower intrinsic viscosity values for the same total molecular weight, and a much smaller Mark–Houwink exponent ($a = 0.39$, Table 1):

$$[\eta]_{\text{star}} = (1.42 \times 10^{-4}) M_w^{0.68} \quad (8)$$

$$[\eta]_{\text{HBPS}} = (6.45 \times 10^{-4}) M_w^{0.39} \quad (9)$$

In previous experimental and simulation studies on dendrimers and hyperbranched polymers, the compact, globular shape was consistent with unusually low values of $[\eta]$ and the Mark–Houwink exponent (a).^{37,44–48} It appears that the low values for $[\eta]$ and a in our samples also suggest that the synthesis procedure resulted in compact starlike hyperbranched polymers. In fact, the Mark–Houwink exponent in our study agrees well with what is found in recent studies on hyperbranched polyesteramides²³ and poly(methyl methacrylate).²⁴

Experimental measurements of ratios of intrinsic viscosity of stars with varying number of arms, to linear polymers of the same total molecular weight are summarized by Mishra and Kobayashi.¹⁸ Under conditions of good solvent, they offer the following expression for prediction of such ratio for symmetric stars with $f \geq 6$ arms:

$$H = [\eta]_{\text{Star}}/[\eta]_L = 10^{[0.36 - 0.80 \log(f)]} \quad (10)$$

Our measurements of H for symmetric stars are shown in Figure 5, along with a fit suggested by eq 10. Experimental data for symmetric stars seem to follow this trend satisfactorily. For HBPS, ratio $[\eta]_{\text{HBPS}}/[\eta]_L$ is plotted against the "average" number of arms, f , evaluated from the column 5 of Table 1. Good agreement with the empirical fit given above, further validates the estimate of the number of HBPS branches, initially obtained from the synthesis and SEC³ procedure.

On the basis of intrinsic viscosity measurements (eq 1), we obtain viscometric radii R_{η} for HBPS, symmetric PS stars, and corresponding values of linear polymers. They are utilized to estimate the change in hydrodynamic dimensions of branched systems through the analysis of the h factor. It appears that R_{η} of HBPS is only about 50% of the values for linear PS of the same total molecular weight (Table 2). One may notice that 5K- and 10K-HBPS possess relatively higher branch densities ($f \approx 50$) than the rest of HBPS, yet the degree by which their hydrodynamic radius is reduced due to the presence of numerous branches is nearly the same as that of less branched HBPS, suggesting that in highly dense HBPS molecular shrinkage is in competition with partial expansion due to "axial" orientation.

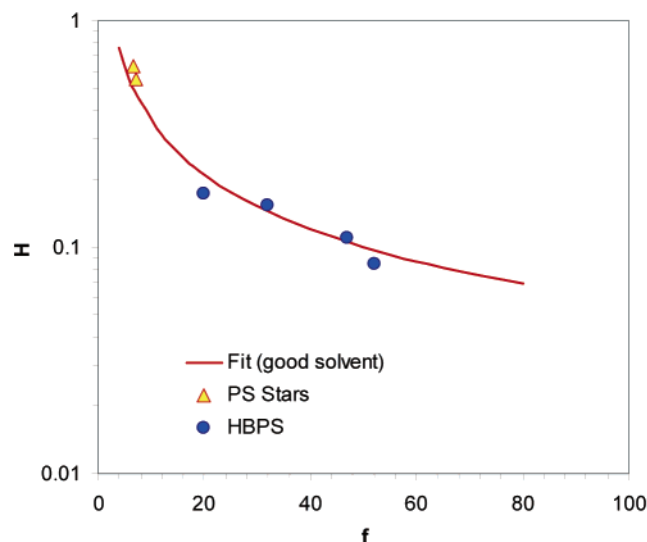


Figure 5. Verification of the number of branches of HBPS and symmetric stars. Empirical fit of H values under conditions of good solvent is used (eq 10, solid curve). Triangles represent experimental values for symmetric stars obtained in THF (good solvent), and circles show corresponding quantities for HBPS in THF.

A different picture is found for symmetric stars with only eight arms. When evaluating ratios of hydrodynamic radii of star polystyrenes to corresponding linear polymers, h values of 0.8 were observed (Table 2). This result is in a very good agreement with work of Striolo and co-workers, on symmetric PS stars with same number of branches.⁴⁹ For the same arm molecular weight ($\sim 10\,000$), the HBPS appears to have a higher R_h (Table 2, Column 3), perhaps indicating that in the HBPS (with the higher branch density) there is some chain stretching near the core.

It is well-known that there is a number of technical difficulties with the estimation of radius of gyration, when it is very small ($\langle R_g^2 \rangle^{1/2} < 15\text{ nm}$).²³ Therefore, $\langle R_g^2 \rangle^{1/2}$ values of only two HBPS were successfully measured using the smallest possible multiple-angle analysis (Table 2). The corresponding quantities for linear polymers were obtained with much higher accuracy resulting in the scaling of $\langle R_g^2 \rangle^{1/2}$ vs M_w according to

$$\langle R_g^2 \rangle^{1/2} = (1.48 \times 10^{-2}) M_w^{0.58} \quad (11)$$

Parameters of this fit are in a good agreement with the work of Nakamura and co-workers, who also reported reduction in the exponent from 0.6 to 0.46 for polystyrene combs in good solvent.⁵⁰ To establish similar power-law dependence for our samples is difficult, since the variation of branch lengths for the same branch density in these polymers is limited. To get an idea about how the dimensions of HBPS molecules compare to that of linear PS and polystyrene microgels in the study of McGrath et al.,⁵¹ experimentally obtained radii of gyration of the three HBPS systems are shown in Figure 6 when plotted against weight-average molecular weight. When data for 10K- and 20K-HBPS are added in Figure 6, it appears that the dimensions of these HBPS are roughly twice as big as the microgels but about three times smaller than linear molecules of equal molecular weight.

In their work on the analysis of chain dimensions of multiarmed polyisoprene stars, Bauer and co-workers

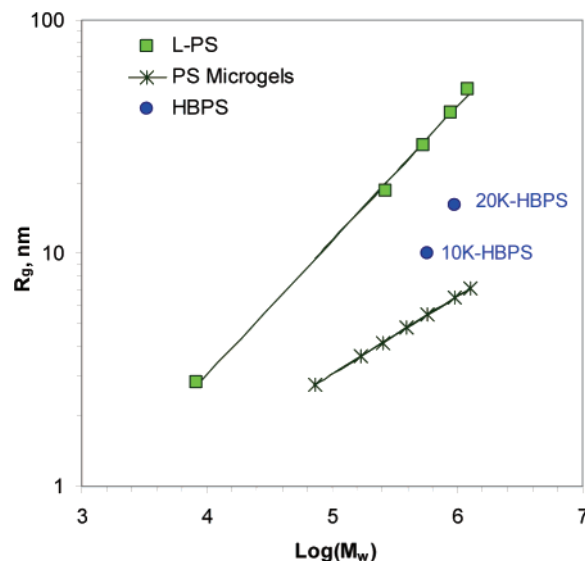


Figure 6. Comparison of the size of HBPS (circles) to that of linear polystyrenes in our study (squares with fitted line) and polystyrene microgels (crosses with fitted lines) in work of McGrath et al.⁵¹ Note that the tentative slope in molecular dependence of radius of gyration for HBPS is physically unrealistic, suggesting 20K-HBPS is significantly less branched than 10K-HBPS.

have extensively described scaling laws for the radius of gyration and hydrodynamic radius.⁵² On the other hand, similar work was conducted by Roovers and Comantia, studying dimensions of dendrimers.³⁷ It has been pointed out that depending on the generation number, the (R_h/R_g) ratio would directly reflect the degree of molecular compactness. For linear polymers, symmetric stars with a few arms, and low generation number dendrimers, this ratio would effectively be less than unity, whereas the opposite should be observed for dendrimers with high generation number and symmetric stars with high branch functionality. The limiting value in the latter case would be the condition of equal-density sphere, for which $(R_h/R_g) = (5/3)^{1/2}$.⁵³ The molecular compactness of our polymers are plotted with those of PI and PS stars (Figure 7). Along with the typical behavior of rigid sphere shown by upper dashed line ($\rho = 1.291$), another limiting behavior characterizing linear PS chains in our study is represented by the lower dashed line. The degree of molecular compactness, ρ for the present linear PS ($f = 2$) is appreciably lower than 1 ($\rho \approx 0.76$), and is in excellent agreement with the previous works.⁵⁴ To portray additional evidence for increasing compactness with increasing f , some experimental data on polyisoprene (PI) and polystyrene stars were added in Figure 7 from literature.⁵² Clearly, when the number of arms was risen from $f = 2$ to $f \approx 50$, the increase in ρ -factor up to values of rigid spheres is seen, suggesting formation of very compact structures with somewhat penetrable (or soft) shells. Both values of ρ for 10K- and 20K-HBPS are very close to unity (Table 2). Therefore, these HBPS values may be viewed as relatively compact spheres with a soft shell.

To compare the melt behavior of HBPS with stars and dendrimers, the molecular weight dependence of zero-shear rate viscosity (η_0) is plotted in Figure 8. The viscosity data are obtained from the dynamic measurements of viscoelastic properties of HBPS, which are addressed elsewhere.^{1,10} In this double-logarithmic plot, linear polystyrenes demonstrate an anticipated type of

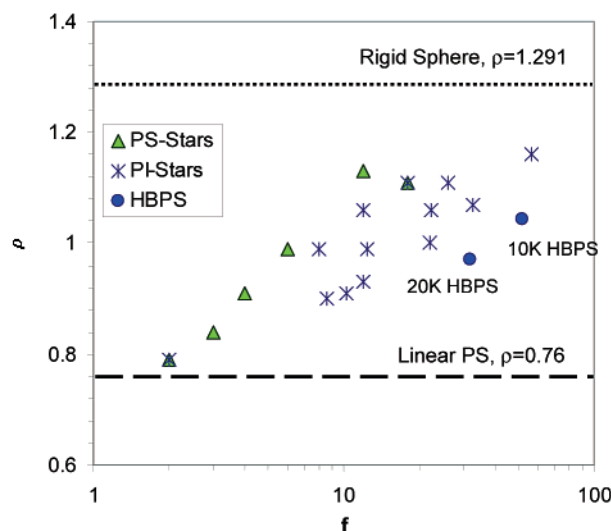


Figure 7. Measure of compactness of HBPS through estimation of the ρ factor. The upper dashed line shows the behavior of impenetrable spheres ($\rho = 1.291$), and the lower dashed line characterizes the linear polymers in our study with $\rho = 0.76$. Triangles show data on PS stars and star symbols show PI stars in work of Roovers et al.^{29,40} and Fetters et al.⁵² Rhombs represent experimentally measured ρ for HBPS in our study.

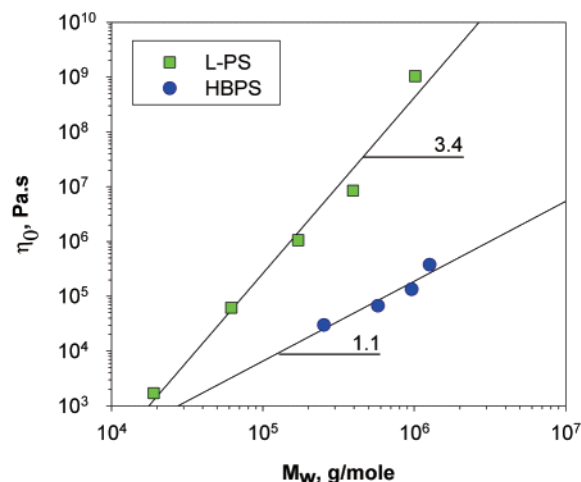


Figure 8. Molecular weight dependence of the zero-shear rate viscosity of L-PS (squares) and HBPS (circles) at $T_{ref} = 150^\circ\text{C}$. Dashed lines represent linear fits to experimental data.

molecular weight dependence, showing a slope of approximately 3.4, consistent with that of a well-entangled polymer. However, regardless of the high total molecular weights, HBPS develops a slope of only 1.1, suggesting a lack of entanglement in the present HBPS. This behavior is analogous to dendrimers^{14,45} and other hyperbranched polymers.⁵⁵ It should also be noted that even though the scaling of η_0 with molecular weight is similar to that of unentangled polymers, the absolute value is much higher than that observed for linear unentangled polymers of corresponding arm molecular weight, as indicated from Figure 8, and is consistent with what has been observed for other star polymers. The branches of HBPS are shorter than the critical molecular weight of PS (36 kg/mol), with only exception of 50K-HBPS ($M_{br} = 50$ kg/mol). Therefore, it appears that both the high branch functionality and the branch length are contributing to the lack of entanglement shown by the zero-shear viscosity. Even though 50K-HBPS has the lowest branch density and has a branch

molecular weight larger than M_c , its viscosity is higher than what would have been predicted from the molecular weight dependence of the rest of HBPS. This polymer shows a “hint” of the entanglement type of response (i.e., appearance of the estimated plateau modulus).¹

Conclusions

The role of branch architecture and branch density on the solution behavior in highly branched polymers is explored in this study. Using anionic polymerization, hyperbranched polystyrenes with fixed branch lengths were synthesized. The branch functionality, f , for the HBPS estimated from the synthetic procedure is in good agreement with the GPC and intrinsic viscosity data. Our SEC³ data suggest that these HBPS may be viewed as star-core polymers with a high branching density.

Using SEC³ and multiangle light scattering, the $[\eta]$, R_g , R_η , and additionally η_0 values for linear, symmetric star, and the HBPS were measured, and the shrinking factors g , h , and ρ for the HBPS were estimated. Our results show that the HBPS have a significantly lower intrinsic viscosity, Mark-Houwink exponent, and hydrodynamic radius, compared to a linear PS of the same total molecular weight. These data suggest that the present HBPS may be viewed as compact soft-sphere-like structures. An analysis of the h shrinking factor allows us to distinguish between the effect of branching on the reduced hydrodynamic volume, from the effect of molecular perturbation of chain conformations, which influences the excluded volume of HBPS. Such analysis was thoroughly performed earlier by Bauer and co-workers on symmetric stars,⁵² agreement with which we find in our work even in the case of HBPS. The examples of this are 5K- and 10K-HBPS, which possess the highest branch density, yet their h factors are on the same order as that of 20K- and 50K-HBPS. It appears that HBPS with short branches ($M_{br} = 5000$ and $10\,000$ g/mol $\ll M_c$) may undergo strong preferential stretches near the center of a molecule, which are, in the present case, thought to be accountable for the partial molecular expansion. When the degree of branching is high, and the branch length is less than M_c , steric hindrance prevents formation of the entanglements, resulting in a linear dependence of zero-shear rate viscosity vs molecular weight.

In the following paper,¹ the melt rheology and the orientation behavior of these highly branched polymers will be compared with the linear and symmetric stars, to understand how the branch density is manifested in the flow behavior.¹

Acknowledgment. Funding from NSF (R.M.K.) (CAREER Award DMR-#9876221), 3M nontenured faculty grant (R.M.K.), and WSU-Institute of Manufacturing Research (Graduate Research Assistantship for S.B.K.) are greatly appreciated.

References and Notes

- (1) Kharchenko, S. B.; Kannan, R. M.; Cernohous, J. J.; Venkataramani, S. Role of Architecture on the Rheology and Orientation Behavior of Linear, Star, and Hyperbranched Polymer Melts. 2. Rheology and Orientation. *Macromolecules* **2003**, *36*, 407.
- (2) Graessley, W. W.; Roovers, J. *Macromolecules* **1979**, *12*, 5.
- (3) Carella, J. M.; Gotro, J. T.; Graessley, W. W. *Macromolecules* **1986**, *19*, 659.
- (4) Struglinski, M. J.; Graessley, W. W.; Fetters, L. J. *Macromolecules* **1988**, *21*, 783.

- (4) Ball, R. C.; McLeish, T. C. B. *Macromolecules* **1989**, *22*, 1911.
- (5) McLeish, T. C. B.; Milner, S. T. *Adv. Polym. Sci.* **1999**, *143*, 1999, 195 and references therein.
- (6) Vogtle, F.; Wehner, W.; Buhleier, E. *Synthesis* **1978**, *55*, 155.
- (7) Kim, Y. H. U.S. Pat. 4857630, 1987.
- (8) Tomalia, D. A.; Baker, H.; Dewald, J.; Hall, M.; Kallos, G.; Martin, S.; Roech, J.; Ryder, J.; Smith, J. *Polym. J.* **1985**, *17*, 177.
- (9) Hawker, C. J.; Frechet, J. M. J. *J. Am. Chem. Soc.* **1990**, *112*, 7638.
- (10) Malmstrom, E.; Hult, A. J. *Macromol. Sci. Rev. Macromol. Chem. Phys.* **1997**, *37*, 555.
- (11) Hult, A.; Johansson, M.; Malmstrom, E. *Adv. Polym. Sci.* **1999**, *143*, 1.
- (12) Kharchenko, S. B.; Kannan, R. M.; Cernohous, J. J.; Babu, G. N.; Venkataramani, S. *J. Polym. Sci.* **2001**, *39*, 2562.
- (13) Hanselmann, R.; Holter, D.; Frey, H. *Macromolecules* **1998**, *31*, 3790.
- (14) Kim, Y. H. *J. Polym. Sci., Part A* **1998**, *36*, 1685.
- (15) Newkome, G. R.; Yao, Z.-Q.; Baker, G. R.; Gupta, V. K. *J. Org. Chem.* **1985**, *50*, 2003.
- (16) Frechet, J. M. J. *J. Macromol. Sci.—Pure Appl. Chem.* **1996**, *A33*, 1399.
- (17) Webster, O. W. U.S. Pat. 4417034, 1983.
- (18) Webster, O. W.; Sogah, D. Y. EP 68887, 1983.
- (19) Sogah, D. Y.; Webster, O. W. *J. Polym. Sci., Polym. Lett. Ed.* **1983**, *21*, 927.
- (20) Webster, O. W. *Makromol. Chem., Macromol. Symp.* **1990**, *33*, 133.
- (21) Kim, Y. H.; Webster, O. W. *J. Am. Chem. Soc.* **1990**, *112*, 4592.
- (22) Kim, Y. H.; Webster, O. W. *Polym. Prepr., Am. Chem. Soc. Div. Polym. Chem.* **1988**, *29* (2), 310.
- (23) Sunder, A.; Heinemann, J.; Frey, H. *Chem.—Eur. J.* **2000**, *6*, 2499.
- (24) Voit, B. Voit, B. *J. Polym. Sci., Part A* **2000**, *38*, 2505.
- (25) Mishra, M. K.; Kobayashi, S. *Star and Hyperbranched Polymers*; Marcel Dekker: New York, 1999.
- (26) Zimm, B. H.; Stockmayer, W. H. *J. Chem. Phys.* **1949**, *17*, 1301.
- (27) Stockmayer, W. H.; Fixman, M. *Ann. N. Y. Acad. Sci.* **1953**, *57*, 334.
- (28) Flory, P. J. *J. Am. Chem. Soc.* **1952**, *74*, 2718.
- (29) Burchard, W. *Adv. Polym. Sci.* **1983**, *48*, 1.
- (30) Simon, P. F. W.; Muller, A. H. E.; Pakula, T. *Macromolecules* **2001**, *34*, 1677.
- (31) Gelade, E. T. F.; Goderis, B.; de Koster, C. G.; Meijerink, N.; van Benthem, R. A. T. M. *Macromolecules* **2001**, *34*, 3552.
- (32) Merino, S.; Brauge, L.; Caminade, A.-M.; Majoral, J.-P.; Taton, D.; Gnanou, Y. *Chem.—Eur. J.* **2001**, *7*, 14, 3095.
- (33) Mourey, T. H.; Turner, S. R.; Rubinstein, M.; Frechet, J. M. J.; Hawker, C. J.; Wooley, K. L. *Macromolecules* **1992**, *25*, 2401.
- (34) Voit, B. I. *Acta Polym.* **1995**, *46*, 87.
- (35) Appelhans, D.; Komber, H.; Voigt, D.; Haussler, L.; Voit, B. I. *Macromolecules* **2000**, *33*, 9494.
- (36) Prosa, Ty, J.; Bauer, B. J.; Amis, E. J.; Tomalia, D. A.; Scherrenberg, R. *J. Polym. Sci., Part B: Polym. Phys.* **1997**, *35*, 2913.
- (37) Roovers, J. E. L.; Bywater, S. *Macromolecules* **1972**, *5*, 385.
- (38) Bauer, B. J.; Fetters, L. J. *J. Rubber Chem. Technol.* **1978**, *50*, 407.
- (39) Huber, K.; Burchard, W.; Fetter, L. J. *Macromolecules* **1984**, *17*, 541.
- (40) Larson, R. *Constitutive Equations for Polymer Melts and Solutions*; Butterworths: Boston, MA, 1988.
- (41) Doi, M.; Edwards, S. F. *The Theory of Polymer Dynamics*; Clarendon Press: Oxford, England, 1988.
- (42) Roovers, J.; Martin, J. E. *J. Polym. Sci.* **1989**, *27*, 2513.
- (43) Vlassopoulos, D.; Pakula, T.; Fytas, G.; Roovers, J.; Karatasos, K.; Hadjichristidis, N. *Europhys. Lett.* **1997**, *39*, 617.
- (44) Pakula, T.; Vlasopoulos, D.; Fytas, G.; Roovers, J. *Macromolecules* **1998**, *31*, 8931.
- (45) Roovers, J.; Comantia, B. *Adv. Polym. Sci.* **1999**, *142*, 179.
- (46) Bauer, B. J.; Hadjichristidis, N.; Fetters, L. J.; Roovers, J. E. L. *J. Am. Chem. Soc.* **1980**, *102*, 2410.
- (47) Mazur, J.; McCrackin, F. *Macromolecules* **1977**, *10*, 326.
- (48) Iatrou, H.; Siakali-Kioulafa, E.; Hadjichristidis, N.; Roovers, J.; Mays, J. *J. Polym. Sci. Part B: Polym. Phys.* **1995**, *33*, 1925.
- (49) Roovers, J. *Macromol. Symp.* **1997**, *121*, 89.
- (50) Roovers, J.; Toporowski, P. M. *J. Polym. Sci.: Polym. Phys. Ed.* **1980**, *18*, 1907.
- (51) Roovers, J.; Zhou, L.-L.; Toporowski, P. M.; van der Zwan, M.; Iatrou, H.; Hadjichristidis, N. *Macromolecules* **1993**, *26*, 4324.
- (52) Young, R. J.; Lovell, P. A. *Introduction to Polymers*, 2nd ed.; Chapman & Hall: New York, 1991.
- (53) Wood-Adams, P. M.; Dealy, J. M.; deGroot, A. W.; Redwine, O. D. *Macromolecules* **2000**, *33*, 7489.
- (54) Ferry, J. D. *Viscoelastic Properties of Polymers*; John Wiley & Sons: New York, 1980; Chapter 13, p 374.
- (55) Roovers, J. *J. Polym. Sci.* **1999**, *37*, 1329.
- (56) Frechet, J. M. *Science* **1994**, *263*, 1710.
- (57) Ishizu, K.; Takahashi, D.; Takeda, H. *Polymer* **2000**, *41*, 6081.
- (58) Schappacher, M.; Deffieux, A. *Macromolecules* **2000**, *33*, 7371.
- (59) Lyulin, A. V.; Adolf, D. B.; Davies, G. R. *Macromolecules* **2001**, *34*, 3783.
- (60) Striolo, A.; Prausnitz, J. M.; Bertuccio, A. *Macromolecules* **2000**, *33*, 9583.
- (61) Nakamura, Y.; Wan, Y.; Mays, J. W.; Iatrou, H.; Hadjichristidis, N. *Macromolecules* **2000**, *22*, 8323.
- (62) McGrath, K. J.; Roland, C. M.; Antonietti, M. *Macromolecules* **2000**, *33*, 8354.
- (63) Bauer, B. J.; Fetters, L. J.; Graessley, W. W.; Hadjichristidis, N.; Quack, G. F. *Macromolecules* **1989**, *22*, 2337.
- (64) Khasat, N.; Pennisi, R. W.; Hadjichristidis, N.; Fetters, L. J. *Macromolecules* **1988**, *21*, 1100.
- (65) Yamakawa, H. *Modern Theory of Polymer Solutions*; Harper and Row: New York, 1971.
- (66) Freed, K. F.; Wang, S.-Q.; Roovers, J.; Douglas, J. F. *Macromolecules* **1988**, *21*, 2219.
- (67) Sendjarevic, I.; Liberatore, M. W.; McHugh, A. J. *J. Rheol.* **2001**, *45*, 1245.

MA0256486